Single-cell heterogeneity and the growth laws

Leandra Brettner[1]*, Kerry Geiler-Samerotte[1,2]

[1]Biodesign Institute Center for Mechanisms of Evolution, Arizona State University, Tempe, Arizona, USA
[2]School of Life Sciences, Arizona State University, Tempe, Arizona, USA
*corresponding author: leandra.brettner@asu.edu

ABSTRACT

Previous work has suggested that the number of ribosomes in a cell is optimized to maximize cell growth given nutrient availability. The resulting correlation between ribosome number and growth rate, called a “growth law”, appears to be independent of which nutrient limits growth rate and is apparent in many organisms. Growth laws have had a powerful impact on many biological disciplines, having fueled predictions about how organisms evolve to maximize their growth and models about how cells regulate their growth. Problematically, the growth law is rarely studied at the single-cell level. While populations of fast-growing cells tend to have more ribosomes than populations of slow-growing cells, it is unclear whether individual cells tightly regulate their ribosome content to match their environment. Here we use recent ground-breaking single-cell RNA sequencing techniques to study the growth law at the single cell level in two different microbes, *S. cerevisiae* (a single-celled yeast and eukaryote) and *B. subtilis* (a bacterium and prokaryote). In both species, we find enormous variation in the ribosomal content of single cells that is not predictive of growth rate. Fast-growing populations of cells include cells showing transcriptional signatures of slow growth and stress, as do some cells with the highest ribosome content we survey. These results demonstrate that single-cell ribosome levels are not finely tuned to match population growth rates or nutrient availability and encourage expansion of models that predict how growth rates evolve or are regulated to consider single-cell heterogeneity.

INTRODUCTION

Growth laws describe robust correlations between cell growth and other phenotypes[1–4]. Perhaps one of the most well-studied growth laws pertains to the relationship between cell growth and the ribosome[5,6]. Numerous studies have shown that faster growing populations of cells possess more ribosomes[7–9]. This makes intuitive sense as ribosomes make most of the components that cells need to grow and replicate. However, ribosomes are expensive, being composed of many proteins and rRNA molecules, and comprising a large portion of the transcriptome[10–14]. Thus, cell populations are thought to tightly optimize ribosome levels to match their environment[15,16]. This tight optimization has been demonstrated at the transcriptional level; ribosomal as well as many other growth-supporting transcripts respond in concert to changes in nutrient abundance or environment quality[17,18], sometimes within minutes[7]. The optimization of ribosome levels to match cell growth rate has been observed across diverse growth-limiting environments[19,20] and organisms[7–9,21,22], most often manifesting as a linear correlation[1,2,8].

This tight coupling of population growth rate and ribosome levels has allowed important advances across diverse fields. It has enabled predicting the growth of cells from the levels of their ribosomes or other growth-supporting molecules[7,9,23,24], provided insights about the regulatory circuits that allow cells to fine-tune their growth to match their environments[16,19,25], and suggested trends governing how cells across the tree of life should evolve to optimize ribosome utilization[1,2,26,27]. More generally speaking, the idea that cells optimize their transcriptome and proteome to maximize their "cellular economy" has been a guiding principle across diverse biological disciplines[3,4,11].

Although literature pertaining to the growth law discusses the ribosomal content "per cell" and models how single cells regulate their ribosome content[1,2,8,25], the relationship between ribosomes and growth has most often been studied in aggregate. It has historically been difficult to measure the number of ribosomes in a single, tiny microbial cell. Alternatively, there are several well-established ways to macerate a large number of cells, measure the total amount of ribosome content in their lysate, typically as a mass-to-mass ratio of RNA to protein, and how that quantity changes across similarly sized populations of cells growing at different rates. Numerous studies following this approach have shown that a population's average ribosome level changes in lock step with its growth rate. But taking the average can mask heterogeneity[28]. For example, this may obscure subpopulations of cells that follow different evolutionary strategies to maximize fitness, such as cells that maintain high levels of ribosomes despite growing slowly[29,30]. This in turn may blind us to the existence of alternate regulatory circuits that allocate resources in different ways in certain cell populations or environments. These circuits may represent different evolutionary solutions to the problem of maximizing fitness given resource availability. In sum, perhaps we are missing interesting biology by averaging away these signals.

Here we investigate heterogeneity in ribosome levels across single cells by utilizing data we and others recently generated by using a novel high-throughput method (Split Pool Ligation based Transcriptome sequencing, SPLiT-seq) that enables the sequencing of transcriptomes of individual microbial cells[31,32]. While more common cell isolation-based approaches have difficulty sequencing microbial cells due to their small size and unique anatomies, SPLiT-seq overcomes these limitations and allows capture of thousands of RNA transcripts per microbial cell[31,32]. We implemented SPLiT-seq using random hexamer primers that recover rRNA, in addition to the

typically used polydT primers that bias recovery towards mRNA. This enables us to use these data to study how the ribosomal abundance of microbial cells changes as growth rate changes. We used data surveying roughly 8,200 haploid and diploid yeast cells (*S. cerevisiae*) and 5,300 bacterial cells (*B. subtilis*), sampled at different times – and thus varying growth rates – across the growth curve (**Figure 1a**). The cells averaged 6,390 or 2,644 rRNA reads per cell (for yeast and bacteria respectively).

Contrary to the expectation that cells optimize their ribosome content to match their growth rate, we find enormous heterogeneity in single-cell ribosome levels across genetically identical cells that have the same access to growth-supporting nutrients. When we focus on nutrient conditions supporting fast growth, cells do not exclusively have high ribosomal content or other transcriptional signatures of fast growth. Similarly, when we focus on only those cells with the most ribosomes, these cells do not exclusively possess transcriptional signatures of fast growth. Indeed, some show transcriptional signatures of stress. We conclude that, while the ribosomal content of cell populations is a strong predictor of population growth rate[7,9,23,24], the ribosomal content of a single cell appears to be a poor predictor. These results call for further study of the growth law, in particular, reconciliation of ideas about optimization of the cellular economy with data from single-cell studies revealing widespread heterogeneity.

RESULTS AND DISCUSSION

Single-cell ribosome levels do not correlate with population growth rate. Either yeast (*S. cerevisiae*)[31] or bacteria (*B. subtilis*)[32] were grown in batch culture and sampled over time starting when populations were at or near steady state growth and ending as the cells were exhausting their nutrients. Cell counts or optical density were measured over time to create growth curves for each population of cells (**Figure 1a,** gray lines). To track the rate at which the populations of cells were growing at each time point, we calculated a sigmoidal function to fit the growth curve and then took the log2 ratio between the adjacent data points (**Figure 1a,** black lines). We used these calculations to estimate the instantaneous growth rate of each population we study (**Figure 1b-c,** horizontal axes). These cells sampled at each time point were also used to perform single-cell RNA sequencing via Split-Pool Ligation based transcriptomics sequencing (SPLiT-seq)[31,32]. We used these transcriptional data to calculate the ribosomal content of, on average, 2,045 and 683 single cells per sample for yeast and bacteria, respectively (**Figure 1b,** vertical axes). As expected, based on the growth law, there is a strong correlation between the average amount of ribosomal RNA in a population of cells and that population's instantaneous growth rate (**Figure 1b**). In both yeast and bacteria, we find that population growth rate explains 94% and 69% of variance in average rRNA abundance respectively when using a linear model (**Figure 1b,** R-squareds). The non-linearity in slow-growing *B. subtilis* populations where ribosomal content appears to be less responsive to changes in nutrient content has been observed for other bacterial species as well[22].

However, this correlation breaks down at the single-cell level where the population growth rate explains 5% and 12% of variance in single-cell rRNA abundance in yeast and bacteria respectively (**Figure 1c,** R-squareds). Even in conditions when cells are flush with nutrients and the population is doubling at the fastest rate we survey, there is massive variation in ribosome content across cells spanning more than two orders of magnitude (**Figure 1c**). This is 25 times

as much variation as we observe on average across timepoints (**Figure 1b**). If all this variation arises from sampling noise, then we would expect noise to be highest in slow-growing populations of cells that have, on average, fewer ribosomal transcripts. However, that is not the case (**Figures 1 & 2**). This high level of heterogeneity seems unexpected if single cells optimize their ribosome levels to maximize their growth rate given the nutrient availability.

Single-cell growth rate heterogeneity does not explain heterogeneity in rRNA abundance. One hypothesis to explain the large variation in single-cell rRNA abundance is that it is due to corresponding heterogeneity in single-cell growth rates. In some ways, this hypothesis is consistent with the growth law because it asserts that every single cell's ribosome content is tightly correlated to its own rate of growth. If this were true, then single-cell growth rates should be most heterogeneous when single-cell ribosome abundances are also most variable. Interestingly, we observe that rRNA abundance heterogeneity (as calculated by the mean normalized standard deviation, or coefficient of variation σ/μ) correlates positively to the population's growth rate. That is to say, fast growing populations of cells sampled when nutrients are most abundant have the highest heterogeneity in rRNA counts in both yeast and bacteria (**Figure 2a**). This positive correlation between ribosome heterogeneity and population growth rate appears to be consistent with at least one previous study in another organism[22]. To understand whether heterogeneity in ribosomal content reflects heterogeneity in single-cell growth rates, we sought to find if heterogeneity in single-cell growth rates is positively correlated with the population growth rate.

Here, we investigate how heterogeneity in single-cell growth rates varies with population growth rate using two different approaches. First, we infer single-cell growth rates from gene expression profiles, or the genes and quantities of expression detected in each cell. Previous work reports correlation values between gene expression and growth rate for the majority of *S. cerevisiae* genes[9,23]. Genes for which expression is higher during faster growth have positive correlation values, and those for which expression is higher during slow growth have negative correlations. We used the associative values in Brauer et al. 2008[9] to weight the gene expression in our single cells and calculate an arbitrary predicted growth rate using the formula described in the Methods.

Next, we used these inferred values to ask if variation in single-cell growth rates positively correlates with the population growth rate, as does variation in single-cell ribosome levels (**Figure 2b**). To do so, we took the coefficient of variation of the predicted single-cell growth rates for each population growth rate as a measure of growth rate heterogeneity. However, unlike the rRNA abundance heterogeneity (**Figure 2a**), the heterogeneity in single-cell growth rate negatively correlates with population growth rate in yeast. This may suggest that variation in the growth of individual cells is not responsible for the spread of rRNA abundance we observe.

However, these measurements may suffer from the same issue we observe in rRNA abundance–that is, they were estimated using values taken from the mean of a bulk population. Thus, we also performed a second analysis to confirm our results that does not rely on inference from scRNAseq data. For this analysis, we used an independent data set of single-cell *S. cerevisiae* growth measurements where the growth of thousands of yeast microcolonies was monitored over time using high-throughput microscopy[33]. We aggregated all microcolonies and averaged the growth rate for each timepoint to generate a proxy for population growth rate. Like

our data, the mean growth rate generally decreases with time as nutrients are consumed. We then again calculated the heterogeneity using the coefficient of variation of the individual growth rates of the microcolonies as stratified by time point. Like our gene expression predicted growth rate data, the heterogeneity of single-cell growth rates declines as the population average increases (**Figure 2c**). These negative correlations are the opposite of what we see in the rRNA data.

In sum, we show that single-cell growth rates are most heterogeneous in slow-growing populations of cells (**Figure 2b-c**), but single-cell ribosome levels are most heterogeneous in fast-growing populations of cells (**Figure 2a**). These results do not support the hypothesis that single-cell growth rate variation is driving the heterogeneity we observe in rRNA abundance. Next, we further analyzed the heterogeneity in single-cell ribosomal content by using data from the rest of the transcriptome.

Transcriptional analysis reveals heterogeneous cell types even within steady-state growth. Heterogeneity in and of itself seems potentially inconsistent with the spirit of the growth law, which is based on the idea that cells have evolved to tightly optimize their cellular economy[3,4,11]. We were particularly surprised to see high heterogeneity in single-cell ribosome levels in our fastest growing populations of cells because these populations were collected at or near steady-state growth. Previous works demonstrating ribosomal growth laws are often performed on populations of cells growing at steady state[9,15,16,25]. These studies make the implicit assumption that steady-state populations are homogeneous such that it is possible to model the number of ribosomes (or other molecules) per cell from population-level measurements[25]. This assumption is consistent with a model in which cells are all similarly striving to optimize their levels of ribosomes to match the maximum growth rate supported by the nutrient concentration. However, it is within our steady-state timepoints that we paradoxically observe the most rRNA abundance variability. Therefore, we examined the rest of the transcriptome in these fastest growing populations of cells to understand to the extent their other behaviors support or contradict this supposition of uniformity.

Contrary to expectations, there are variant expression patterns between cells when our populations are in, or close to, steady state (**Figure 3**). In both yeast and bacteria, we observe cells that show the expression signatures associated with faster growth–genes related to ribosome production, translation, carbon utilization, RNA processing, and cell replication. However, we also find cells that show signs of classic stress responses–general stress proteins, genes related to respiration and the TCA cycle and mitochondrial proteins, trehalose metabolism[34], and low glucose conditions (**Figure 3**). We wondered if perhaps the cells expressing stress-related transcripts represent those that are growing slower due to stressors like DNA damage or cell aging. However, when we compare the cells mounting a transcriptional response characteristic of “growth” vs. “stress”, we see a near complete overlap between the distributions of ribosome abundance (**Figure 3**). This supports our conclusion that it is difficult to predict the growth rate of single cells from rRNA levels or the levels of other transcripts (**Figure 1c**).

Perhaps one explanation for these data is that even our earliest sampled cell populations are not actually in steady state growth, despite having been previously grown at low density for multiple generations in rich media before being transferred into fresh and ample nutrients for the

reported growth curves. But given heterogeneity in ribosome levels increases as we sample closer to steady state (**Figure 2a**), it seems unreasonable to suggest that these diverse transcriptional signatures would disappear had we sampled cells closer to steady state growth. Further, it is important to study the degree to which growth laws break down in environments that are commonly encountered in nature, such as those where nutrient levels are decreasing over time[35]. Indeed, the diverse transcriptional signatures we observe are not restricted to cells growing at or near steady state. Cells expressing growth-responsive and cells expressing stress-responsive transcripts are present in multiple timepoints along the growth curve. Given these two cell types have largely overlapping ribosomal contents (**Figure 3**), it seems difficult to predict a cell's growth behavior from its ribosome levels.

The heterogeneity we observe is consistent with other studies that show single-cell heterogeneity is the rule rather than the exception[28,32–34,36,37]. Though high-throughput single-cell transcriptomics in microbial cells is just emerging, previous work examining the transcriptomes of a small number of cells or higher-throughput studies using fluorescent markers have shown that heterogeneity is incredibly common. For example, previous work suggests that persister cells[38,39], or more generally, slow growing cells that have unusually high stress tolerance[34], exist even in fast-growing cell populations that have access to high levels of nutrients. Even under conditions of stress, when mounting a transcriptional stress response may mean the difference between life or death, not all cells respond uniformly, or even respond at all[40,41].

Single-cell heterogeneity sometimes reflects bet-hedging, in other words, a simultaneous display of multiple evolutionary strategies to prepare for an unknown future[34,42]. For example, an alternate evolutionary strategy, besides maximizing growth rate, may involve harboring excess ribosomes to prepare for conditions that require increased translation[29,35,43,44]. Another strategy may involve expressing stress-responsive, rather than growth-responsive transcripts, to prepare for unexpected and unfavorable environments[34,38,39]. But cell-to-cell heterogeneity could also simply result from unavoidable processes like expression stochasticity, DNA damage, or aging[37,45,46]. Whatever the underlying cause of the heterogeneity, our observation that single cells do not seem to optimize their ribosome content (or their transcriptomes) to match their nutrient level may call for additional work reconciling the growth law with single-cell heterogeneity and the knowledge that cells can maximize fitness via diverse evolutionary strategies.

Cells with the most ribosomes do not all have transcriptional signatures of faster growth, and cells with the fewest ribosomes do not all have signatures of slower growth. To further investigate whether the ribosomal content of a cell is optimized to match its rate of growth, we decided to compare "apples to apples," so to speak. We ordered the cells by their ribosome abundance from least to greatest across all time points. If ribosomes are the dominant signatures of growth rate, we would expect the cells with the most ribosomes to have uniform growth signals in their transcriptomes, and the cells with the least ribosome abundance to show signs of stress or slow growth.

We separated the cells into four quartiles and used Louvain clustering to investigate any subpopulations that might be present within each quartile. Differential expression analysis on the identified subpopulations revealed that, within each quartile, cells segregated by signatures of growth and stress (**Figure 4a**). Contrary to our expectations given the growth law, the cells with the highest number of rRNAs do not all have transcriptomes suggestive of fast growth (**Figure**

4a.i-ii). Similarly unexpected under the assumptions of the growth law was that some cells with the fewest ribosomes still appear to be employing transcriptional programs associated with a growth-oriented directive (**Figure 4a,** iii-iv).

In yeast, the "growth" clusters (**Figure 4a;** green) are defined by the expression of genes involved in glycolysis, ribosome biogenesis, and translation. The "stress" clusters (**Figure 4a,** gray) show upregulated gene expression of heat stress, osmotic stress, and protein misfolding stress pathways. In bacteria, in the "growth" clusters (**Figure 4a,** green) we see differential expression of similar translation and ribosome biogenesis pathways, and also operons involved in the import and digestion of preferred carbon sources. The "stress" cluster (**Figure 4a,** gray) is defined by expression of genes such as sporulation initiation, bacteriocin production, and surfactin production. Additionally, in both organisms we see an intermediate cluster of cells (**Figure 4a,** light green) that are shifting from glycolysis and preferred carbon digestion to the TCA cycle and operons for the import and digestion of less desirable carbon sources such as short chain fatty acids, and in *B. subtilis*, the lichenan pathway[47]. The salient observation is that all clusters (stress and growth) are present in both cells with the most ribosomes (**Figure 4a,** i-ii) and cells with the least ribosomes (**Figure 4a,** iii-iv). This observation persists even when we normalize ribosome abundance by mRNA abundance and suggests that each single cell's ribosome content is not tightly optimized to match the maximum growth rate supported by its environment.

An alternate interpretation of the growth law might posit that cells with the highest or the lowest ribosome content include those with non-optimal numbers of ribosomes given their environment. In this case, one might expect cells that have an intermediate ribosomal content to express growth-responsive, rather than stress-responsive transcripts. However, we see both cell types persist for cells with intermediate amounts of ribosomes as well. Further even after we sort by ribosome abundance, the strongest signature in the clustering is the sample time point (**Figure 4b**). This suggests that a cell in a quartile of ribosomes from early in the growth curve and a cell with comparable ribosomes from later on are not most essentially defined by their ribosome abundance. Perhaps this result appears obvious in retrospect, but if ribosomes and growth activities were intrinsically linked as the growth law suggests, then the null assumption would be that these cells should be alike. Seemingly, having similar amounts of rRNA does not make cells similar at the rest of the transcriptional level. Thus, our findings advise caution when equating ribosome level to growth state, at least at the single-cell level.

METHODS

Growth curve and single-cell sequencing data. Growth curve single-cell sequencing data for *Saccharomyces cerevisiae* and *Bacillus subtilis* were obtained from previously published works by L. Brettner and others[31,32]. However, the saved *S. cerevisiae* sample libraries were re-sequenced on the NovaSeqX platform with paired end reads for a total of 300 cycles. This provided further and deeper coverage than what was reported in Brettner et al. 2024[31]. Sequencing and processed data for *S. cerevisiae* can be found through GEO at accession number GSE251966 and for *B. subtilis* at GSE151940. Additional processed data and analysis scripts can be found at the Open Science Framework: https://osf.io/kjfbz/.

Cell density curve and growth rate curve calculations. The cell densities reported in cells/mL for yeast and OD600 for bacteria, and timepoints in hours were used to calculate a sigmoidal curve through a nonlinear weighted least-squares estimate in R (nls function). The model was fitted to the function for a sigmoid as follows (**Figure 1a,** gray lines).

$$cell\ density = \frac{L}{1 + e^{-k(t-t_0)}}$$

Where L is the saturation density, t0 is the half maximal time, and k is the slope. The data points from these models were then used to fit the growth rate curve in generations per hour using a log2 ratio between adjacent points normalized to the time increment as follows (**Figure 1A,** black lines).

$$\frac{generations}{hr} = \log_2 \frac{\left(\frac{cell\ density[i]}{cell\ density[i-1]}\right)}{\Delta t}$$

A sigmoidal function might not be the best approximation of growth under very low densities and early in the growth curve as it assumes continuous exponential growth and cannot incorporate any kind of lag phase. This might explain why the maximal estimated yeast growth rate is slightly higher than typically reported in the literature (~1.05 generations/hour compared to ~0.75 generations/hour). However, the absolute value is of little importance, and instead the shape of the curve and the relative relationships between the points are what impact the relevant downstream models (eg. the goodness of linear fits, R^2).

Single-cell RNA seq data processing, rRNA abundance calculations, and mRNA normalization. Sequencing reads were aligned to the R64 s288c genome for *Saccharomyces cerevisiae* from NCBI or the ASM904v1.45 genome for *Bacillus subtilis* from EnsemblBacteria and sorted by barcode using STARsolo[48]. As both the yeast and bacterial genomes have significant sequence homology, especially within rRNA genes, we enabled the uniform multimapping algorithm within STARsolo to keep overlapping reads. This outputted gene-by-barcode matrices representing the detected gene counts for every cell. To remove empty and low gene detection barcodes, we applied the “knee” detection filter previously described in Brettner et al. 2024[31]. These quality-thresholded gene-by-barcode matrices were then converted to the R datatype, Seurat Objects, using the Seurat R package for further analyses[49].

rRNA genes were identified using the Saccharomyces Genome Database (SGD)[50] and SubtiWiki[51]. Counts from these genes were then aggregated to calculate an rRNA abundance for each cell. While single-cell RNA sequencing data is typically highly sparse for mRNA, the minimum combined rRNA counts detected in one cell in these data were well above 500 reads. As scRNAseq data normalization methods are designed for sparse, low count data, we used the raw total rRNA counts in all ribosome abundance analyses to avoid unnecessary data distortion[52].

Normalization, scaling, nearest neighbor calculations, clustering, and differential expression analyses were performed similar to the tutorial provided by the Satija Lab[53] on mRNA datasets with the rRNA removed. As rRNA typically makes up greater than 90% of the detected RNA reads and clustering is relative, keeping it in made for skewed clustering analyses that obscured some of the interesting biological behaviors.

Estimating single-cell growth rates from transcriptional data. Gene expression and growth rate correlation values were obtained from Brauer et al. 2008[9]. These values were used to weight normalized and scaled mRNA expression for each cell using the following formula with rRNA genes removed.

$$single\ cell\ estimated\ growth\ rate = \frac{\sum_{i}^{all\ genes} Brauer\ correlation_i * gene\ expression_i}{total\ detected\ expression}$$

This equation produces an arbitrary, unitless number. The more positive the number, the more the transcriptome of that cell is indicative of growth-related expression and vice versa.

Within timepoint analyses (Figure 3). We bioinformatically separated out the transcriptomes of the exponentially growing cells from the sample timepoints that best approximate steady-state growth (**Figure 1a**). These also happen to be the timepoints with the highest mean rRNA abundance and the most recovered cells. In yeast, this sample corresponds to the first timepoint when the cells are at $9.2*10^6$ cells/mL and growing at an estimated 1.05 generations/hour. In bacteria, we chose the timepoint when the cells were at OD600 of 1.0 and a growth rate of 1.22 generations/hour. This corresponds to the second timepoint in the bacterial series, but the difference in growth rate from the first timepoint at OD600 0.5 is only approximately -0.03 generations per hour. More importantly, this second timepoint has almost 2.5 times more recovered cells, significantly increasing the resolution of any subpopulations detected via clustering methods. Additionally, this second timepoint also has the highest mean rRNA abundance.

We then applied a Louvain clustering algorithm to these cells with a low enough resolution to only produce 2 to 3 clusters. We then performed a differential expression analysis on these clusters and categorized the top 20 positive genes in each using SGD[50], Metascape[54], or SubtiWiki[51]. We used these categorizations to classify each cluster, and found they dichotomized by growth and stress related genes. We sorted out the cells by barcode for each cluster and used violine plots to visually compare the rRNA means and distributions.

"Apples to apples" rRNA quartile analyses (Figure 4). We first calculated the minimum and maximum rRNA abundances for each timepoint and found the largest minimum and smallest maximum. The largest minimum and smallest maximum were used to create a bandwidth filter to allow for more direct comparisons of cells with similar rRNA amounts with representatives from each timepoint. Cells within this bandwidth were sorted by rRNA from least to greatest and quartiles were calculated. We then applied the same Louvain clustering to cells from each quartile and analyzed the gene categorizations and ontologies as above.

FIGURES

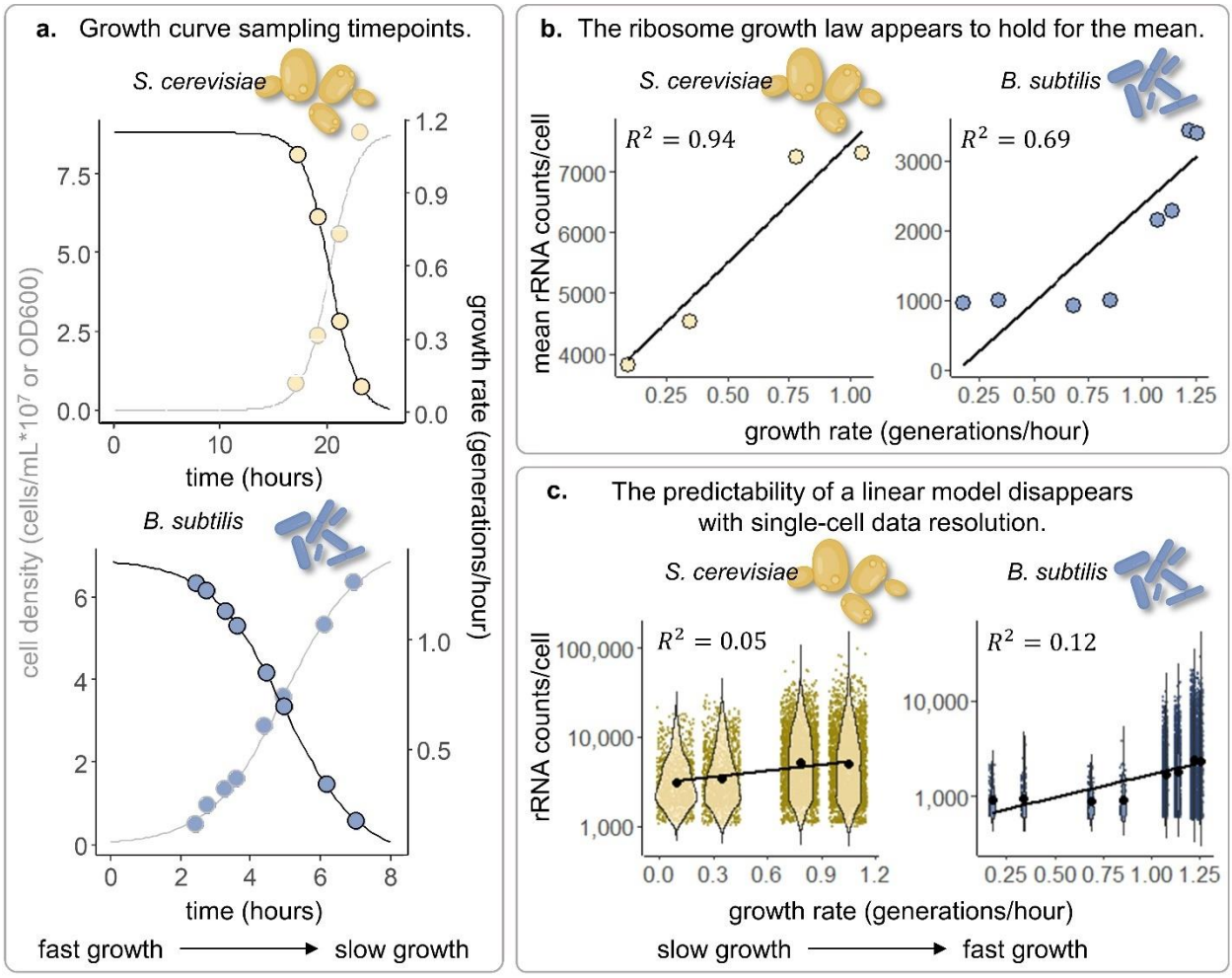

Figure 1. Population average ribosome levels correlate with population growth rates, but single-cell ribosome levels do not. a.) Cell density (black) given in cells/mL*10^7 in yeast and OD600 in bacteria and growth rate in generations per hour (gray) against time in hours. Yeast were sampled at 0.92, 2.7, 5.7, and 8.6*10^7 cells per milliliter. Bacteria were sampled at OD600 0.5, 1.0, 1.3, 1.6, 2.0, 3.6, 5.3, and 6.0. Yeast and bacteria cartoon icons were created using Biorender[55]. **b.)** mean detected rRNA counts per cell versus the population growth rate in generations per hour. Trend lines and R^2s were calculated by applying a linear regression model to the mean data points in R. **c.)** rRNA counts for all datapoints represented as violin distributions. Means (black dots) and trendlines are the same as in b. R^2s were calculated by applying a linear regression model to the entire dataset.

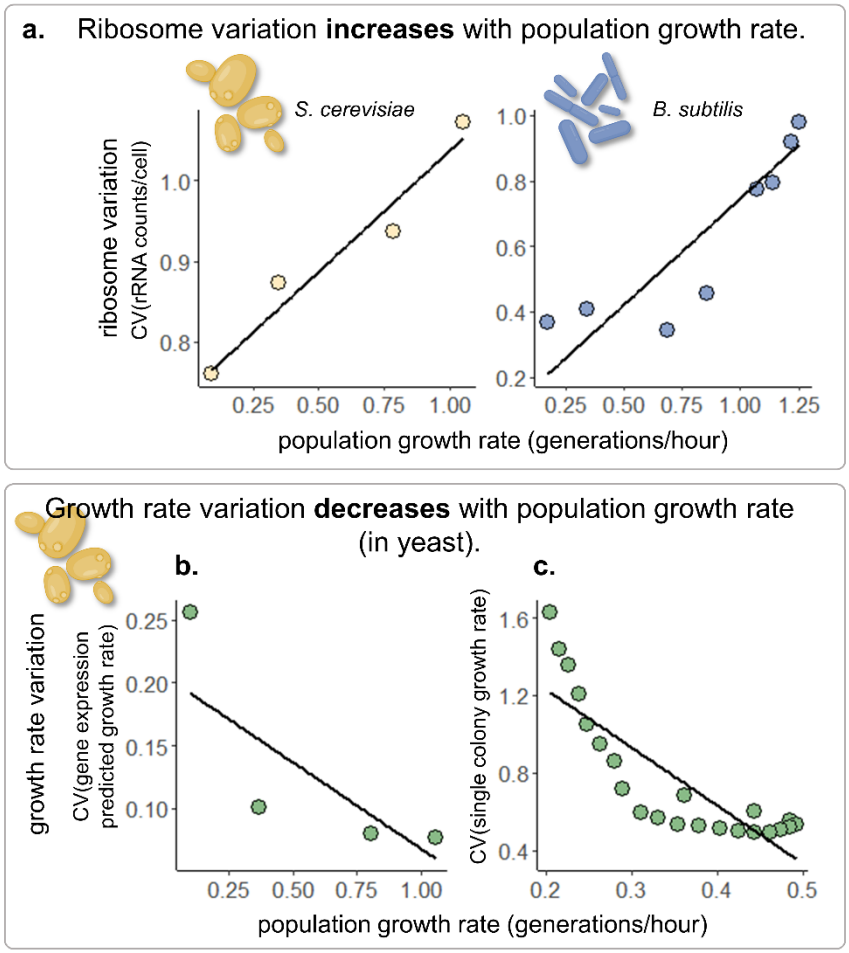

Figure 2. Single-cell ribosome heterogeneity trends opposite to single-cell growth rate heterogeneity. a.) Coefficient of variation (σ/μ) of ribosome counts for cells in each timepoint against population growth rate. **b.)** Coefficient of variation of single-cell growth rates estimated using gene expression (Methods) for cells in each timepoint against population growth rate. **c.)** Coefficient of variation of single microcolony growth rates against the average growth rate for each imaging time[33]. Trendlines are shown to indicate the direction of correlation with population growth rate.

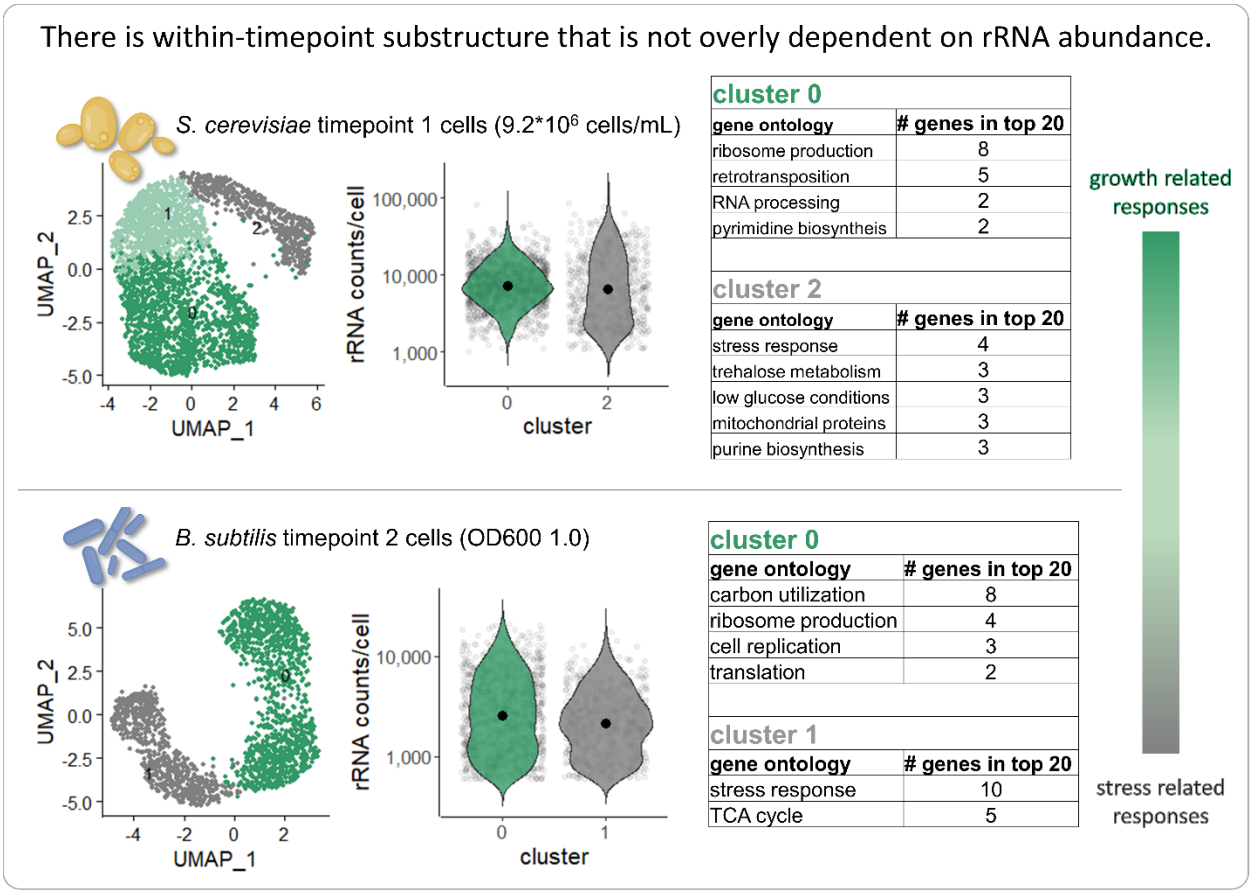

Figure 3. UMAP embeddings for cells from the first timepoint in yeast ($9.2*10^6$ cells/mL) and second timepoint in bacteria (OD600 1.0) colored by Louvain cluster. Ribosome counts per cell distributions for growth gene expression dominated (green) and stress gene expression dominated (gray) clusters. Gene ontologies for the top 20 differentially expressed genes in each cluster that appear for two or more genes.

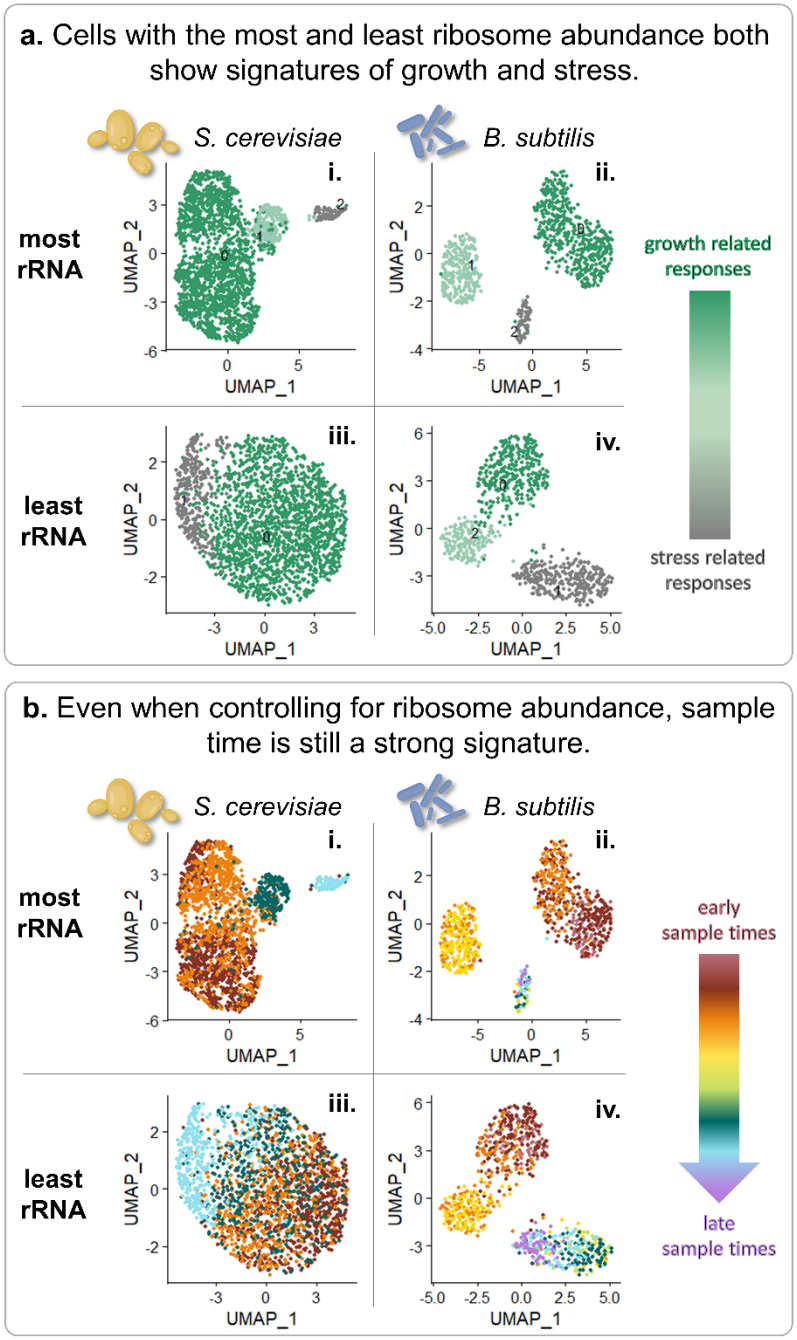

Figure 4. Cells show differential subpopulations and signatures of sample timepoint despite having similar ribosome levels a.) UMAP embeddings of cells from the most (i-ii) and least (iii-iv) rRNA abundance quartiles colored by Louvain cluster. **b.)** UMAP embeddings of cells from the most (i-ii) and least (iii-iv) rRNA abundance colored by sample timepoint.

REFERENCES

1. Lynch, M. Evolutionary Scaling Laws in Cell Biology. in *Evolutionary Cell Biology: The Origins of Cellular Architecture* (2022).
2. Lynch, M. Cell Growth and Division. in *Evolutionary Cell Biology: The Origins of Cellular Architecture* (2023).
3. Golan, O. *et al.* Models of growing cells. in *Economic Principles in Cell Biology* 117–134 (2024).
4. Kremling, A., Liebermeister, W., Noor, E. & Wortel, M. Metabolism in states of maximal enzyme efficiency. in *Economic Principles in Cell Biology* 107–116 (2024).
5. Schaechter, M., Maaloe, O. & Kjeldgaard, N. O. Dependency on medium and temperature of cell size and chemical composition during balanced grown of Salmonella typhimurium. *J Gen Microbiol* **19**, 592–606 (1958).
6. Scott, M. & Hwa, T. Bacterial growth laws and their applications. *Current Opinion in Biotechnology* **22**, 559–565 (2011).
7. Airoldi, E. M. *et al.* Predicting Cellular Growth from Gene Expression Signatures. *PLOS Computational Biology* **5**, e1000257 (2009).
8. Scott, M., Gunderson, C. W., Mateescu, E. M., Zhang, Z. & Hwa, T. Interdependence of Cell Growth and Gene Expression: Origins and Consequences. *Science* **330**, 1099–1102 (2010).
9. Brauer, M. J. *et al.* Coordination of growth rate, cell cycle, stress response, and metabolic activity in yeast. *Mol Biol Cell* **19**, 352–367 (2008).
10. Maaløe, O. Regulation of the Protein-Synthesizing Machinery—Ribosomes, tRNA, Factors, and So On. in *Biological Regulation and Development: Gene Expression* (ed. Goldberger, R. F.) 487–542 (Springer US, Boston, MA, 1979). doi:10.1007/978-1-4684-3417-0_12.
11. Warner, J. R. The economics of ribosome biosynthesis in yeast. *Trends Biochem Sci* **24**, 437–440 (1999).
12. Wilson, D. N. & Nierhaus, K. H. The Weird and Wonderful World of Bacterial Ribosome Regulation. *Critical Reviews in Biochemistry and Molecular Biology* **42**, 187–219 (2007).
13. Ali, A. *et al.* Adaptive preservation of orphan ribosomal proteins in chaperone-dispersed condensates. *Nat Cell Biol* **25**, 1691–1703 (2023).
14. Pelava, A., Schneider, C. & Watkins, N. J. The importance of ribosome production, and the 5S RNP–MDM2 pathway, in health and disease. *Biochem Soc Trans* **44**, 1086–1090 (2016).
15. Scott, M., Klumpp, S., Mateescu, E. M. & Hwa, T. Emergence of robust growth laws from optimal regulation of ribosome synthesis. *Mol Syst Biol* **10**, 747 (2014).
16. Bosdriesz, E., Molenaar, D., Teusink, B. & Bruggeman, F. J. How fast-growing bacteria robustly tune their ribosome concentration to approximate growth-rate maximization. *The FEBS Journal* **282**, 2029–2044 (2015).
17. Keren, L. *et al.* Promoters maintain their relative activity levels under different growth conditions. *Molecular Systems Biology* **9**, 701 (2013).
18. Gasch, A. P. *et al.* Genomic Expression Programs in the Response of Yeast Cells to Environmental Changes. *MBoC* **11**, 4241–4257 (2000).
19. Towbin, B. D. *et al.* Optimality and sub-optimality in a bacterial growth law. *Nat Commun* **8**, 14123 (2017).

20. Wang, Q. & Lin, J. Environment-specificity and universality of the microbial growth law. *Commun Biol* **5**, 1–9 (2022).
21. Zavřel, T. *et al.* Quantitative insights into the cyanobacterial cell economy. *eLife* **8**, e42508 (2019).
22. Matamouros, S. *et al.* Growth-rate dependency of ribosome abundance and translation elongation rate in Corynebacterium glutamicum differs from that in Escherichia coli. *Nat Commun* **14**, 5611 (2023).
23. Slavov, N. & Botstein, D. Coupling among growth rate response, metabolic cycle, and cell division cycle in yeast. *MBoC* **22**, 1997–2009 (2011).
24. Tadmor, A. D. & Tlusty, T. A Coarse-Grained Biophysical Model of E. coli and Its Application to Perturbation of the rRNA Operon Copy Number. *PLOS Computational Biology* **4**, e1000038 (2008).
25. Wu, C. *et al.* Cellular perception of growth rate and the mechanistic origin of bacterial growth law. *Proceedings of the National Academy of Sciences* **119**, e2201585119 (2022).
26. Maitra, A. & Dill, K. A. Bacterial growth laws reflect the evolutionary importance of energy efficiency. *Proceedings of the National Academy of Sciences* **112**, 406–411 (2015).
27. Bruggeman, F. J., Planqué, R., Molenaar, D. & Teusink, B. Searching for principles of microbial physiology. *FEMS Microbiology Reviews* **44**, 821–844 (2020).
28. Geiler-Samerotte, K. A. *et al.* Quantifying Condition-Dependent Intracellular Protein Levels Enables High-Precision Fitness Estimates. *PLOS ONE* **8**, e75320 (2013).
29. Metzl-Raz, E. *et al.* Principles of cellular resource allocation revealed by condition-dependent proteome profiling. *eLife* **6**, e28034 (2017).
30. Kafri, M., Metzl-Raz, E., Jonas, F. & Barkai, N. Rethinking cell growth models. *FEMS Yeast Research* **16**, fow081 (2016).
31. Brettner, L., Eder, R., Schmidlin, K. & Geiler-Samerotte, K. An ultra high-throughput, massively multiplexable, single-cell RNA-seq platform in yeasts. *Yeast* **41**, 242–255 (2024).
32. Kuchina, A. *et al.* Microbial single-cell RNA sequencing by split-pool barcoding. *Science* **371**, (2021).
33. Ziv, N., Siegal, M. L. & Gresham, D. Genetic and Nongenetic Determinants of Cell Growth Variation Assessed by High-Throughput Microscopy. *Mol Biol Evol* **30**, 2568–2578 (2013).
34. Levy, S. F., Ziv, N. & Siegal, M. L. Bet hedging in yeast by heterogeneous, age-correlated expression of a stress protectant. *PLoS Biol* **10**, e1001325 (2012).
35. Korem Kohanim, Y. *et al.* A Bacterial Growth Law out of Steady State. *Cell Reports* **23**, 2891–2900 (2018).
36. Ackermann, M. A functional perspective on phenotypic heterogeneity in microorganisms. *Nat Rev Microbiol* **13**, 497–508 (2015).
37. Elowitz, M. B. Stochastic Gene Expression in a Single Cell. *Science* **297**, 1183–1186 (2002).
38. Balaban, N. Q., Merrin, J., Chait, R., Kowalik, L. & Leibler, S. Bacterial Persistence as a Phenotypic Switch. *Science* **305**, 1622–1625 (2004).
39. Lewis, K. Persister cells, dormancy and infectious disease. *Nat Rev Microbiol* **5**, 48–56 (2007).
40. Gasch, A. P. *et al.* Single-cell RNA sequencing reveals intrinsic and extrinsic regulatory heterogeneity in yeast responding to stress. *PLOS Biology* **15**, e2004050 (2017).

41. Munsky, B., Li, G., Fox, Z. R., Shepherd, D. P. & Neuert, G. Distribution shapes govern the discovery of predictive models for gene regulation. *Proceedings of the National Academy of Sciences* **115**, 7533–7538 (2018).
42. Grimbergen, A. J., Siebring, J., Solopova, A. & Kuipers, O. P. Microbial bet-hedging: the power of being different. *Curr Opin Microbiol* **25**, 67–72 (2015).
43. Kafri, M., Metzl-Raz, E., Jona, G. & Barkai, N. The Cost of Protein Production. *Cell Rep* **14**, 22–31 (2016).
44. Eguchi, Y. *et al.* Estimating the protein burden limit of yeast cells by measuring the expression limits of glycolytic proteins. *eLife* **7**, e34595 (2018).
45. Chao, L., Chen, C. K., Shi, C. & Rang, C. U. Spatial and temporal distribution of ribosomes in single cells reveals aging differences between old and new daughters of Escherichia coli. *eLife* **12**, (2023).
46. Raj, A. & van Oudenaarden, A. Nature, nurture, or chance: stochastic gene expression and its consequences. *Cell* **135**, 216–226 (2008).
47. Tobisch, S., Glaser, P., Krüger, S. & Hecker, M. Identification and characterization of a new beta-glucoside utilization system in Bacillus subtilis. *J Bacteriol* **179**, 496–506 (1997).
48. Kaminow, B., Yunusov, D. & Dobin, A. STARsolo: accurate, fast and versatile mapping/quantification of single-cell and single-nucleus RNA-seq data. 2021.05.05.442755 Preprint at https://doi.org/10.1101/2021.05.05.442755 (2021).
49. Hao, Y. *et al.* Integrated analysis of multimodal single-cell data. *Cell* **184**, 3573-3587.e29 (2021).
50. Cherry, J. M. *et al.* Saccharomyces Genome Database: the genomics resource of budding yeast. *Nucleic Acids Res* **40**, D700-705 (2012).
51. Pedreira, T., Elfmann, C. & Stülke, J. The current state of SubtiWiki, the database for the model organism Bacillus subtilis. *Nucleic Acids Research* **50**, D875–D882 (2022).
52. Church, S. H., Mah, J. L., Wagner, G. & Dunn, C. W. Normalizing need not be the norm: count-based math for analyzing single-cell data. *Theory Biosci.* **143**, 45–62 (2024).
53. Getting Started with Seurat. https://satijalab.org/seurat/articles/get_started.html.
54. Zhou, Y. *et al.* Metascape provides a biologist-oriented resource for the analysis of systems-level datasets. *Nat Commun* **10**, 1523 (2019).
55. Created with BioRender.com.